

Effect of Collective Flavor Oscillations on the Diffuse Supernova Neutrino Background

Sovan Chakraborty^{*,a}, Sandhya Choubey^{†,b}, Basudeb Dasgupta^{‡,c}, Kamales Kar^{*,d}

**Saha Institute of Nuclear Physics,
1/AF Bidhannagar, Kolkata 700064, India*

*†Harish-Chandra Research Institute,
Chhatnag Road, Jhansi, Allahabad 211019, India*

*‡Tata Institute of Fundamental Research,
Homi Bhabha Road, Mumbai 400005, India*

ABSTRACT

Collective flavor oscillations driven by neutrino-neutrino interactions inside core-collapse supernovae have now been shown to drastically alter the resultant neutrino fluxes. This would in turn significantly affect the diffuse supernova neutrino background (DSNB), created by all core-collapse supernovae that have exploded in the past. In view of these collective effects, we re-analyze the potential of detecting the DSNB in currently running and planned large-scale detectors meant for detecting both $\bar{\nu}_e$ and ν_e . We find that the event rate can be different from previous estimates by upto 50%, depending on the value of θ_{13} . The next generation detectors should be able to observe DSNB fluxes. Under certain conducive conditions, one could learn about neutrino parameters. For instance, it might be possible to determine the neutrino mass hierarchy, even if $\theta_{13} \rightarrow 0$.

^a email: sovan.chakraborty@saha.ac.in

^b email: sandhya@hri.res.in

^c email: basudeb@theory.tifr.res.in

^d email: kamales.kar@saha.ac.in

1 Introduction

Observation of neutrino signal from a core-collapse supernova (SN) is expected to contribute significantly towards determination of the neutrino mass hierarchy and the mixing angle θ_{13} . It is also expected to shed light on SN shockwave dynamics and set stringent bounds on the existence of sterile neutrinos. Thus a lot of attention has been devoted to this scenario of resonant neutrino conversions in a SN [1, 2]. The work has focussed on the determination of mass hierarchy and signatures of a non-zero θ_{13} [3, 4], Earth matter effects on the neutrino fluxes when they pass through matter [5, 6, 7], shock wave effects on observable neutrino spectra and their model independent signatures [8]-[13]. Recently, possible interference effects for multiple resonances [14], sterile neutrinos [15], the role of turbulence in washing out shock wave effects [16, 17, 18], and time variation of the signal [19] have also been explored. Observational data on SN neutrinos come only from the SN1987A [20, 21, 22], and while it confirms broad expectations, the small number of events limits our ability to draw detailed inferences.

However, supernovae are relatively rare in our galaxy with an estimated rate of about 1 – 3 per century [23], which prompts consideration of the alternative strategy to detect neutrinos from supernovae that are further away. Neutrinos accumulated in the Universe from all the SN explosions in the past and present epoch form a cosmic background, known as the diffuse supernova neutrino background (DSNB) or supernova relic neutrinos [24, 25, 26]. The expected flux of these DSNB neutrinos depends mainly on the SN rate and the “typical” flavor dependent flux of neutrinos from supernovae.

The SN rate can be either determined directly [27] or from the cosmic star formation rate, which is measured using a variety of ways like galaxy luminosity function of rest-frame ultraviolet radiation [28]–[36], far-infrared/sub-millimeter dust emission [37, 38] and near-infrared H α fluorescent line emission [39]–[42] and radio emission [43]. Though these techniques suffer from various ambiguities and complications like dust extinction [44], careful studies have enabled a precise determination of the star formation rate [45].

The typical neutrino flux from a SN on the other hand is not experimentally available. The data from SN1987A do not allow a clean determination of the spectral parameters [46]. So one has to resort to using primary neutrino fluxes predicted using SN simulations. Fluxes predicted by different groups (and sometimes different simulations by the same group) are at considerable variance, because of their different physics input [47, 48]. Additionally, these primary fluxes are further mixed by flavor conversions as they stream through the SN, thus requiring knowledge of not only the typical primary spectra, but also the typical SN density profiles. The emitted neutrino fluxes are therefore ridden with uncertainties at present. However, they could be made precise with more sophisticated simulations or observation of a galactic SN.

Estimation of the DSNB flux has been performed in previous literature, with varying approaches and results [45], [49]–[62]. Most studies have focussed on DSNB detection via $\bar{\nu}_e$ scattering off protons at water Čerenkov detectors [61] and large liquid scintillator detectors [55]. On the other hand, ν_e detection has been considered at a liquid argon detector [63] and at Sudbury Neutrino Observatory (SNO) [64, 65]. In [62], authors have performed a detailed comparative study of ν_e detection in different future large scale observatories – by interaction of ν_e on oxygen in water Čerenkov detectors, on carbon in liquid scintillator detectors and on argon in liquid argon detectors. Experimentally, the best upper limits at 90 % C.L. of $6.8 \times 10^3 \nu_e \text{ cm}^{-2}\text{s}^{-1}$

($25 \text{ MeV} < E_{\nu_e} < 50 \text{ MeV}$) and $1.2 \bar{\nu}_e \text{ cm}^{-2}\text{s}^{-1}$ ($E_{\bar{\nu}_e} > 19.3 \text{ MeV}$) come from the Liquid Scintillation Detector (LSD) [66] and the Super-Kamiokande (SK) detectors [67] respectively. However, stronger bounds can be placed on these fluxes, albeit using somewhat indirect arguments [65, 68]. Some of the theoretical estimates of the DSNB fluxes predict event-rates for $\bar{\nu}_e$ that are tantalizingly close to detection, *e.g.*, the observational upper limit set by the SK collaboration [67]. The prospects for discovery thus seem promising if a large water Čerenkov detector like SK is loaded with 0.02% GdCl_3 [69] or if one or more of the proposed next generation detectors become available.

The study presented in this work removes a common assumption, made for all previous estimates, that neutrino-neutrino interactions are too feeble to cause any flavor conversion. Although these interactions had been studied in previous literature [70]-[75], it has only very recently been appreciated that they induce sizable flavor conversion in supernovae [76, 77]. Motivated by this interesting result, the effects of these neutrino-neutrino interactions have been explored in the context of supernovae, in a series of papers [78]-[92]. The interesting aspect of these conversions is that the neutrinos and antineutrinos of different energies undergo conversions together, and are almost in-phase. Therefore these conversions are referred to as being “collective”. The effect of these interactions becomes negligible beyond the first few hundred kilometers, when the neutrino densities become much lower. The end of these collective effects is marked by a complete (or step-wise) swapping between the flavor spectra of antineutrinos (or neutrinos) for inverted hierarchy (IH) [80, 82, 83]. Further out from the centre of the star, the traditional picture of flavor evolution by Mikheyev-Smirnov-Wolfenstein (MSW) conversion is not changed, except that the primary fluxes emitted at the neutrinosphere undergo the above-mentioned “pre-processing” due to the collective effects. The fluxes emitted by a SN have already been calculated in a three-flavor framework, including the effect of collective oscillations [89]. In this paper, we take these SN neutrino fluxes calculated in [89], the SN rate deduced from the cosmic star formation rate calculated by Beacom *et al.* [45], and the standard Λ -CDM cosmological model [93] as inputs to calculate the DSNB flux. The expected DSNB flux in the case of IH turns out to be quite different from those contained in previous works that disregarded collective effects. Thus the prospects of DSNB detection at antineutrino and/or neutrino detectors are modified. We report the DSNB fluxes and their observability, with and without neutron tagging, at present and proposed detectors. These changed expectations have impact on limits that can be set on non-standard models and interactions of neutrinos as well.

The paper is organised as follows. In Section 2, we outline the dependence on the DSNB event-rate at Earth as a function of the cosmic star formation rate and the primary neutrino fluxes and mention our choice of models for the same. We discuss our choice of detectors. In Section 3, we calculate the event-rates, dependent on the above choices, and present the results. We conclude the paper in Section 4, by summarizing our results and giving an outlook on the impact of these results.

2 DSNB in Terrestrial Detectors

From the early times to the present date, SN explosions have been fairly common events in the Universe. These explosions have injected a large number of neutrinos, with energies of tens of MeV, in the Universe. These neutrinos have created a diffuse background of SN neutrinos known

as diffuse supernova neutrino background. Evidently, the DSNB flux depends on two ingredients:

- The rate of SN explosions $R_{SN}(z)$, as a function of cosmological redshift z .
- The differential flux of neutrinos $F_\nu(E_\nu)$, from a typical core-collapse event at redshift z .

The differential flux of neutrinos $F_\nu(E_\nu)$ depends on the primary neutrino fluxes $F_\nu^0(E_\nu)$, emitted from the neutrinosphere, which get modified due to

- Collective effects, i.e. neutrino-neutrino self interaction, close to the neutrinosphere.
- MSW effects, i.e matter driven neutrino oscillations in the SN mantle and envelope.

The total differential DSNB flux arriving at terrestrial detectors, expressed as the number of neutrinos of flavor ν (where $\nu = \nu_e, \nu_\mu, \nu_\tau$ and antineutrinos are denoted with a bar overhead) arriving per unit area per unit time per unit energy, due to all supernovae in the Universe up to a maximum redshift z_{max} , is

$$F'_\nu(E_\nu) = \int_{z_{max}}^0 \left(dz \frac{dt}{dz} \right) (1+z) R_{SN}(z) F_\nu((1+z)E_\nu) . \quad (1)$$

Here E_ν is the neutrino energy at Earth and $R_{SN}(z)$ is the SN rate per comoving volume at redshift z . For our numerical calculations we have assumed $z_{max} = 7$. Note that the factor $(1+z)$ in the neutrino spectrum $F_\nu((1+z)E_\nu)$ incorporates the redshift of the energy spectrum.

From the Friedmann equation for a flat universe we have

$$\frac{dz}{dt} = -H_0(1+z)(\Omega_m(1+z)^3 + \Omega_\Lambda)^{1/2} . \quad (2)$$

Thus the differential number flux of DSNB is

$$F'_\nu(E_\nu) = \frac{1}{H_0} \int_0^{z_{max}} R_{SN}(z) F_\nu((1+z)E_\nu) \frac{dz}{\sqrt{(\Omega_m(1+z)^3 + \Omega_\Lambda)}} . \quad (3)$$

For the standard Λ -CDM cosmology, we have

$$\Omega_m = 0.3 ; \Omega_\Lambda = 0.7 \text{ and } H_0 = 70 h_{70} \text{ km s}^{-1} \text{ Mpc}^{-1} . \quad (4)$$

Therefore, we only need to know the SN rate $R_{SN}(z)$ and the differential flux of neutrinos $F_\nu(E_\nu)$, from a typical core-collapse event to calculate the DSNB flux at Earth.

2.1 The Cosmic Supernova Rate

The SN rate $R_{SN}(z)$ is related to $R_{SF}(z)$, through the initial mass function $\varphi(m)$, which describes the differential mass distribution of stars at formation [45, 56]. We assume that all stars that are more massive than $8M_\odot$ give rise to core-collapse events and die on a timescale much shorter than the Hubble time, and that the initial mass function $\varphi(m)$ is independent of redshift. This allows us to relate the star formation rate $R_{SF}(z)$ to the cosmic SN rate $R_{SN}(z)$ as

$$R_{SN}(z) = R_{SF}(z) \frac{\int_{8M_\odot}^{125M_\odot} \varphi(m) dm}{\int_{0.1M_\odot}^{125M_\odot} \varphi(m) m dm} . \quad (5)$$

For our estimates, we use the initial mass function from reference [96], i.e.

$$\varphi(m) \propto \begin{cases} m^{-1.50} & (0.1M_{\odot} < m < 0.5M_{\odot}) \\ m^{-2.15} & (m > 0.5M_{\odot}) \end{cases} . \quad (6)$$

Putting the above expression into Eq. (5) we find

$$R_{SN}(z) = 0.0132 R_{SF}(z)M_{\odot}^{-1} . \quad (7)$$

It should be noted that the factor connecting R_{SN} and R_{SF} is quite insensitive to the upper limit of the integrations in Eq. (5).

Recent careful studies on different indicators of the cosmic star formation rate have been used to calculate the R_{SF} and its normalization. We use the cosmic star formation rate per comoving volume, R_{SF} , from the concordance model advocated in [94, 95], which is given by

$$R_{SF}(z) \propto \begin{cases} (1+z)^{3.44} & z < 0.97 \\ (1+z)^{-0.26} & 0.97 < z < 4.48 \\ (1+z)^{-7.8} & 4.48 < z \end{cases} , \quad (8)$$

with the local star formation rate given by

$$R_{SF}(0) = 0.0197 M_{\odot}\text{yr}^{-1}\text{Mpc}^{-3} . \quad (9)$$

This model satisfies the experimental upper limit on DSNB set by SK [67], and hence is known as the concordance model [45, 97].

2.2 Neutrino Fluxes from Core-collapse Supernovae

2.2.1 Primary Neutrino Fluxes

A core-collapse SN is typified by conversion of its gravitational binding energy of about 10^{53} ergs to neutrinos and antineutrinos with energies of tens of MeV. This translates to a total flux of more than 10^{57} per SN explosion. The initial luminosity is about 10^{53} ergs/sec (emitted purely as ν_e in the neutronization burst lasting for about 25 msec), and slowly reduces to about 10^{51} ergs/sec over the following ~ 10 secs. Since the event-rate for DSNB is not very sensitive to the neutronization burst, we can ignore it for our analysis ¹. Subsequently, after the neutronization burst, neutrinos and antineutrinos of all three flavors are emitted with a pinched thermal spectrum, that is conveniently parametrized as [98]

$$F_{\nu}^0(E_{\nu}) = \frac{L_{\nu}^0}{\langle E_{\nu} \rangle^2} \frac{(1 + \zeta_{\nu})^{1+\zeta_{\nu}}}{\Gamma(1 + \zeta_{\nu})} \left(\frac{E_{\nu}}{\langle E_{\nu} \rangle} \right)^{\zeta_{\nu}} \exp \left(-(1 + \zeta_{\nu}) \frac{E_{\nu}}{\langle E_{\nu} \rangle} \right) , \quad (10)$$

where L_{ν}^0 is the luminosity in the flavor ν , $\langle E_{\nu} \rangle$ is the average energy of ν , and ζ_{ν} is the pinching parameter at the neutrinosphere. As a notational convenience, since there is no difference expected between the μ and τ flavors for SN neutrinos, we will refer to them together as x .

¹The neutrinos in the burst phase undergo complicated flavor conversions, particularly for a class of low-density SN with degenerate O-Mg-Ne cores [86, 88, 90, 91]. However, these issues are not likely to be important for DSNB due to the relative smallness of the integrated flux from the burst-phase.

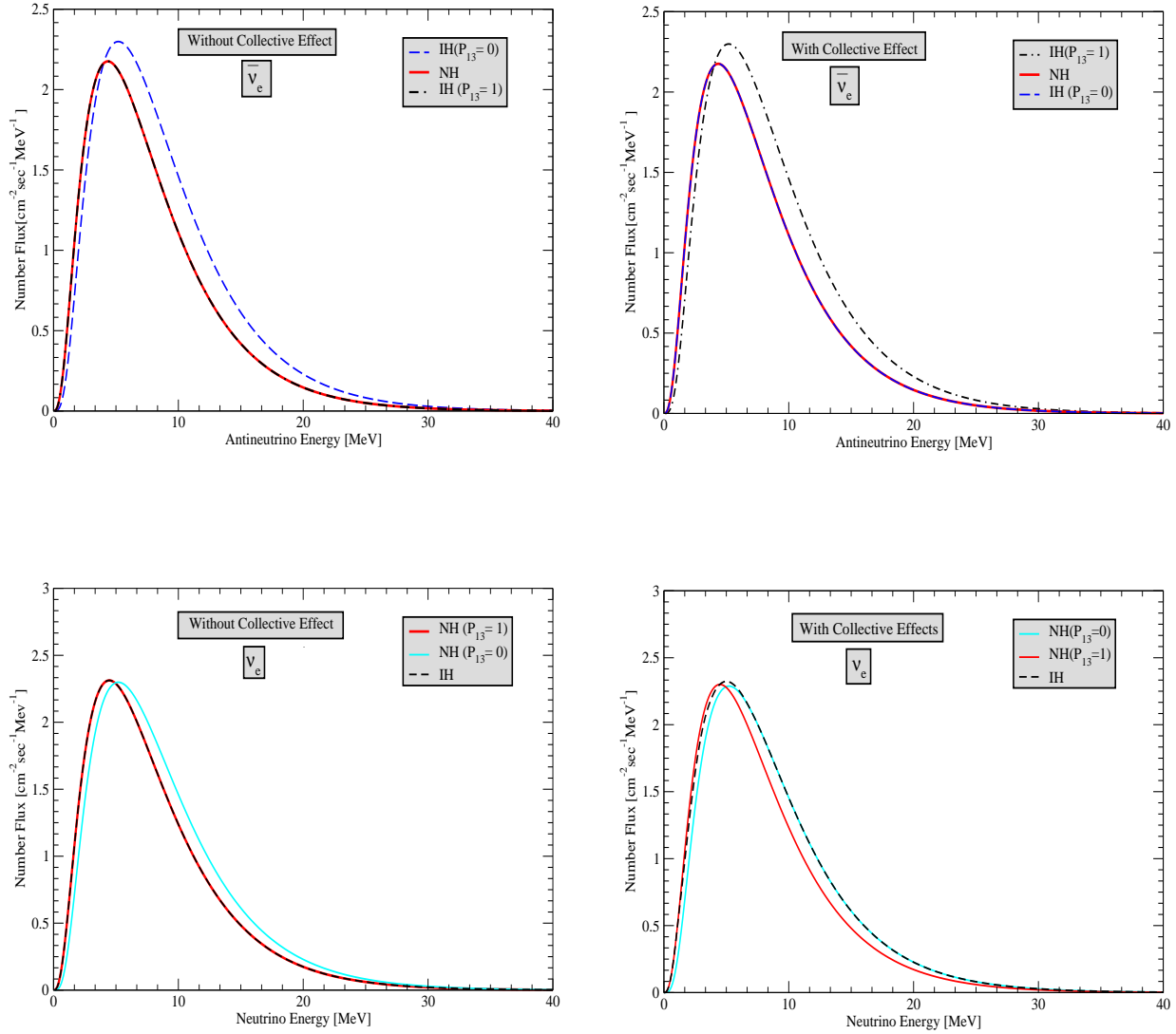


Figure 1: The DSNB flux spectrum arriving at Earth as a function of the (anti)neutrino energy at Earth. The upper panels show the $\bar{\nu}_e$ flux while the lower panels show the ν_e flux. The left panels correspond to the hypothetical case where we have only MSW matter effects in the SN while the right panels correspond to the case where we have both collective as well as MSW-driven flavor transitions. We have assumed that the initial neutrinos are given by the G1 model.

For our study, we take 3 sets of representative values of $\Phi_\nu^0 = L_\nu^0/\langle E_\nu \rangle$, $\langle E_\nu \rangle$ and ζ_ν motivated by SN simulations. One simulation by the Lawrence Livermore group (LL), and two different simulations by the Garching group (G1, G2) have been chosen for our estimates, as shown in Table 1.

Model	$\langle E_{\nu_e} \rangle$	$\langle E_{\bar{\nu}_e} \rangle$	$\langle E_{\nu_x, \bar{\nu}_x} \rangle$	$\frac{\Phi_{\nu_e}^0}{\Phi_{\nu_x}^0}$	$\frac{\Phi_{\bar{\nu}_e}^0}{\Phi_{\bar{\nu}_x}^0}$
LL	12	15	24	2.0	1.6
G1	12	15	18	0.8	0.8
G2	12	15	15	0.5	0.5

Table 1: The parameters of the used primary neutrino spectra models motivated from SN simulations of the Garching (G1, G2) and the Lawrence Livermore (LL) group. We assume $\zeta_{\bar{\nu}_x} = 4$ and $\zeta_{\bar{\nu}_e} = 3$. The total luminosity is chosen to be 3×10^{53} erg.

Note that the LL simulation obtained a large hierarchy $\langle E_{\nu_e} \rangle < \langle E_{\bar{\nu}_e} \rangle < \langle E_{\nu_x} \rangle \approx \langle E_{\bar{\nu}_x} \rangle$, and an almost complete equipartition of energies between flavors. The Garching simulations predict a smaller hierarchy between the average energies, incomplete equipartition, and increased spectral pinching. The differences in the values of these parameters arise from the different physics inputs.

2.2.2 Collective Effects and MSW Transitions

The primary fluxes (at the neutrinosphere) are further processed by collective effects and MSW conversions before they get emitted from the SN².

Near the neutrinosphere, due to the large neutrino density, the neutrino-neutrino interaction energy is very large. This ensures that the neutrinos exhibit synchronized oscillations, i.e. neutrinos of all energies oscillate coherently with the average frequency. These oscillations do not give rise to any effective flavor conversion since the effective mixing angle is highly suppressed due to the large MSW potential. As the neutrinos stream outward, the neutrino density becomes smaller, and bipolar oscillations begin to take place. In the case of IH, these oscillations have large amplitude even for a vanishingly small mixing angle. These oscillations thus can lead to a complete swapping of the $\bar{\nu}_e$ and $\bar{\nu}_x$ spectra. The ν_e and ν_x spectra cannot swap completely, because of lepton number conservation, and the swap occurs only above a certain energy E_c , giving rise to a spectral split [80]. Eventually, beyond a few hundred kilometers, the neutrino-neutrino interaction energy becomes negligible, and collective effects cease to be important.

Thus for normal hierarchy (NH), the collective effects do not affect the fluxes significantly and only MSW conversions are at work. In particular, the MSW resonances affect the ν_e flux, while the $\bar{\nu}_e$ flux remains almost unaffected. For IH, the collective effects swap the ν_e and ν_x above a certain energy E_c , determined by lepton number conservation [80, 90, 91]. Assuming $F_{\nu_x}^0 = F_{\bar{\nu}_x}^0$,

²The detailed picture of collective effects presented herein is valid only for initial spectra that resemble the LL model. However we are interested in seeing the maximum effect that these new effects can cause, and for that purpose it suffices to ignore more complicated features in the spectrum [99] for G1 or G2 like models.

the split-energy E_c is given in the adiabatic approximation by the implicit equation

$$\int_0^{E_c} dE \left(F_{\nu_e}^0(E) - F_{\nu_x}^0(E) \right) = \int_0^\infty dE \left(F_{\nu_e}^0(E) - F_{\bar{\nu}_e}^0(E) \right) . \quad (11)$$

On the other hand for antineutrinos, all $\bar{\nu}_e$ and $\bar{\nu}_x$ are swapped. This pre-processed flux now undergoes the traditional MSW conversions which now affect the $\bar{\nu}_e$ flux, and not the ν_e flux. The neutrinos then travel independently (while getting redshifted) as mass-eigenstates until they reach Earth, wherein they are detected as flavor eigenstates before or after having undergone regeneration inside the Earth. The fluxes of ν_e and $\bar{\nu}_e$ arriving at Earth are given in Table 2, as calculated in [89]. The quantities such as $F_{\nu_\alpha}^0$, are the initial SN neutrino fluxes while F_{ν_α} are the resultant fluxes emerging from the SN at redshift z . The quantities s_{12}^2 and c_{12}^2 stand for

Normal hierarchy	Inverted hierarchy
$F_{\nu_e} = s_{12}^2 \left(P_{13} F_{\nu_e}^0 + (1 - P_{13}) F_{\nu_x}^0 \right) + c_{12}^2 F_{\nu_x}^0$	$F_{\nu_e} = \begin{cases} s_{12}^2 F_{\nu_e}^0 + c_{12}^2 F_{\nu_x}^0 & (E < E_c) \\ F_{\nu_x}^0 & (E > E_c) \end{cases}$
$F_{\bar{\nu}_e} = c_{12}^2 F_{\bar{\nu}_e}^0 + s_{12}^2 F_{\bar{\nu}_x}^0$	$F_{\bar{\nu}_e} = s_{12}^2 F_{\bar{\nu}_x}^0 + c_{12}^2 \left((1 - P_{13}) F_{\bar{\nu}_e}^0 + P_{13} F_{\bar{\nu}_x}^0 \right)$

Table 2: Electron neutrino and antineutrino spectra emerging from a SN. See [89] for a prescription for calculating these final spectra in terms of the primary spectra.

$\sin^2 \theta_{12}$ (taken to be 0.3 for numerical studies) and $\cos^2 \theta_{12}$ respectively and P_{13} is the effective jump probability between the neutrino mass eigenstates due to the MSW resonance(s), and takes a value between 0 and 1. The value of P_{13} is approximately 0 if θ_{13} is large (i.e. $\theta_{13} \gtrsim 6$ degrees) and for smaller values of θ_{13} it has a non-trivial dependence on energy and time, due to multiple resonances [14, 19] and turbulence [16, 17, 18]. However, due to the small number of events, we can probably neglect these sub-leading effects that occur in the small time-window when the shockwave is in the resonance region.

To calculate the DSNB flux at Earth $F'(E_\nu)$, we need to integrate the fluxes in Table 2, correctly redshifted and weighted by the SN rate $R_{SN}(z)$, over redshift z . We show in Fig. 1 the DSNB $\bar{\nu}_e$ (upper panels) and ν_e (lower panels) fluxes arriving on Earth as a function of their (anti)neutrino energy at Earth. We have assumed the G1 model for generating this figure. Note that the energy spectrum gets degraded to smaller energies due to redshift. The left panels show the predicted fluxes when one takes both collective as well as MSW transitions into account. To bring out the contrast with what the situation was earlier, we show in the right panels the predicted fluxes if one does not take collective effects. We can see that for NH the prediction have remained the same even after collective effects were taken, whereas for IH the fluxes are completely different.

2.3 Terrestrial Detectors

An array of existing and planned detectors could catch the DSNB neutrinos. In what follows, we will consider in particular three types of detectors for observing DSNB $\bar{\nu}_e$:

- Water Čerenkov detectors
- Liquid scintillator detectors

- Gadolinium loaded water Čerenkov detectors

Detection of ν_e is more difficult. Both water and liquid scintillator detectors can in principle detect ν_e (as well muon and tau flavored neutrinos and antineutrinos). In water Čerenkov detectors this can be done through neutrino-electron scattering. On the other hand, in liquid scintillators in addition to the neutrino-electron scattering, one can detect ν_e through charged current interaction on ^{12}C , while the other species can be detected through the neutral current interaction on ^{12}C . However, the cross-section for these processes are rather low. Another detector technology that has been proposed for detecting ν_e is to use a high Z material, such as lead (and/or iron), interleaved with scintillators. Among such proposals are the OMNIS/ADONIS projects and the HALO experiment at SNOLAB [100]. Therefore the only chance for detecting the ν_e DSNB would be in a reasonably large

- Liquid argon detector

2.3.1 Water Čerenkov Detectors

An upper bound on the DSNB flux already exists from non-observation of these neutrinos at the SK experiment [67]. Using 1496 days of data with 22.5 kton of fiducial volume, the DSNB flux has been constrained to be less than $1.2 \text{ cm}^{-2} \text{ s}^{-1}$ for $19.3 \text{ MeV} < E_\nu < 30 \text{ MeV}$. SK is still running and could provide further constraint or evidence for DSNB fluxes in the future. Megaton water detectors with fiducial volume in the ballpark of 500 kton have been planned in Japan (Hyper-Kamiokande (HK)) [101], Europe (MEMPHYS) [102], and USA (UNO) [103]. These have been proposed to serve as the far detector for long baseline experiments with powerful accelerator beams. At the same time, they would be used to study neutrinos from natural sources, such as the Sun, atmosphere and nearby supernovae. In particular, they will be useful tools for the observation of DSNB fluxes. While in principle water detectors can detect neutrinos and antineutrinos of all flavors, the easiest to observe is $\bar{\nu}_e$, which is captured on protons via the inverse beta decay process

$$\bar{\nu}_e + p \rightarrow e^+ + n . \quad (12)$$

The emitted positron is observed through the Čerenkov cone produced by it. The “true” positron energy is approximately related to the neutrino energy by $E_\nu - 1.3 \text{ MeV}$. The other types of neutrino species would scatter electrons and thereby could also be detected. However, the cross-section for neutrino-electron scattering is much lower compared to the reaction (12). Therefore, in this paper we will consider the detection of only $\bar{\nu}_e$ in water Čerenkov detectors. The number of events per kton of detector mass is given as

$$N_e = n_T T \int_0^\infty dE_\nu \int_{E_e^{low}}^{E_e^{up}} dE_e F'_\nu(E_\nu) \sigma(E_\nu) R(E_\nu, E_e) , \quad (13)$$

where n_T is the number of protons in a kton of detector mass, T is the total exposure time, E_e the measured positron energy, E_e^{low} is the lower energy threshold, E_e^{up} is the upper energy threshold, $F'_\nu(E_\nu)$ is the DSNB flux at Earth, $\sigma(E_\nu)$ is the cross-section and $R(E_\nu - 1.3, E_e)$ is the energy resolution of the detector. For the energy resolution we assume a Gaussian form

$$R(E_\nu, E_e) = \frac{1}{\sqrt{2\pi}\sigma_E} \exp\left(\frac{-(E_\nu - 1.3 - E_e)^2}{2\sigma_E^2}\right) , \quad (14)$$

where all quantities are given in units of MeV and σ_E is the half width at half maximum (HWHM). For the water Čerenkov detector we use

$$\sigma_E = 0.47\sqrt{(E_\nu(\text{MeV}) - 1.3)}. \quad (15)$$

From Fig. 1 we can see that the DSNB fluxes being redshifted, arrive on Earth predominantly within the energy window $E_\nu = (0 - 35)$ MeV, above which the fluxes are negligible. In this energy range water Čerenkov detectors also register events coming from a myriad of other sources. The main sources of particles which would imitate the DSNB signal include reactor $\bar{\nu}_e$, atmospheric ν_e and $\bar{\nu}_e$, solar ν_e , spallation products induced by cosmic ray muons, and neutrinos from “invisible muons” produced by atmospheric ν_μ and $\bar{\nu}_\mu$. These form a background for the DSNB signal. Events due to reactor $\bar{\nu}_e$ appear roughly in the energy range $(1.8 - 8)$ MeV and these events can be estimated using the information from reactor power and their distances from the detector. In the case of SK for instance, it will be even easier to estimate them since KamLAND [104] directly observes these events. The events due to atmospheric ν_e and $\bar{\nu}_e$ are expected to be lower compared to those due to DSNB below $E \simeq 30$ MeV. Number of events expected from atmospheric ν_e and $\bar{\nu}_e$ can be anyway estimated using the predicted fluxes at these energies and can be included in the analysis of DSNB events. Therefore, these events do not pose a very serious threat to the DSNB analysis. Events due to neutrinos coming from the Sun fall in the energy range $E_\nu \lesssim 20$ MeV and can also be estimated fairly well using the fluxes from the standard solar model as well as from the direct observation of the ^8B fluxes at SNO [105]. These neutrinos can also be identified in the detector from their directionality. Indeed these are the solar neutrino events that SK observes. Therefore, these events do not pose a serious threat to DSNB observation either. The type of events which cause a serious concern are the ones produced from spallation. These events are typically important in the energy window relevant for solar neutrinos, *viz.* for $E \lesssim 20$ MeV. The SK collaboration in their paper [67] show that after suitable cuts there are almost no spallation events above $E_e > 18$ MeV. The lower threshold for the neutrino energy is hence restricted to $E_\nu \geq 19.3$ MeV. The upper limit is taken as 30 MeV.

Despite the different cuts and selection criteria there are two sources of neutrinos which still appear as backgrounds for the DSNB detection. The first has already been discussed above – the ν_e and $\bar{\nu}_e$ events from atmospheric neutrinos. These background events have to be estimated using the detector Monte Carlo. The second type of background comes from “invisible muons” produced by atmospheric ν_μ and $\bar{\nu}_\mu$. These are events where atmospheric ν_μ and/or $\bar{\nu}_\mu$ produce muons with kinetic energy less than 53 MeV, which is the threshold for emitting Čerenkov photons. These muons/antimuons therefore pass undetected and eventually decay into electrons/positrons which are observed by the detector. Estimates for the background due to both these sources have been made by the SK collaboration and can be found in [67].

2.3.2 Liquid Scintillator Detectors

Number of events expected in liquid scintillator are also given by Eq. (13). The predominant reaction is $\bar{\nu}_e$ capture of protons (cf. reaction (12)). The other detection reactions in liquid scintillators are charged and neutral current scattering off electrons, charged current capture of ν_e and $\bar{\nu}_e$ on ^{12}C , neutral current break-up of ^{12}C (see [106] for reactions of ^{12}C)³ and neutral current

³Liquid scintillator detectors can also detect the DSNB ν_e flux by their charged current interactions on ^{12}C [62].

scattering off protons [107]. However, the cross-section for these processes is small, especially at low energies [62, 108, 109], and we reiterate that due to redshift the DSNB fluxes are peaked at lower energies. Therefore, even for liquid scintillators the main detection weapon is the reaction (12). However, compared to the water detectors, liquid scintillators can use the reaction (12) more efficiently, whereby they tag the released neutron. While the positron is detected promptly, the neutron is captured by a proton in the detector, releasing a 2.2 MeV photon which is detected in delayed coincidence after 180 μ s. This results in lesser problems with backgrounds, and liquid scintillator detectors can be used to observe the DSNB neutrino in the broader energy window of $E_\nu = (10 - 25)$ MeV [55].

The other major difference between the liquid scintillator detector and water Čerenkov detector is in the energy resolution, which is much better for the former. The HWHM for liquid scintillator detectors is expected to be better than

$$\sigma_E = 0.1\sqrt{E_\nu(\text{MeV}) - 0.8} . \quad (16)$$

The KamLAND detector in Japan [104] and Borexino in Italy [110] are the currently running liquid scintillator detectors. While KamLAND has a total mass of 1 kton, Borexino is much smaller and comprises of about 300 ton of liquid scintillator. The detectors for the upcoming second generation reactor experiments designed to probe θ_{13} would be far too small to contribute to the study of DSNB neutrinos. However, one could look forward to proposals such as LENA [55] which would be situated in the Pyhasalmi mine in Finland and is expected to have 50 kton of liquid scintillator. Such a big liquid scintillator detector could collect sizable number of DSNB events and prove to be a pivotal player in this game. Another large liquid scintillator detector proposal is the Hanohano project in Hawaii [111].

2.3.3 Gadolinium Loaded Water Čerenkov Detectors

The neutron released in the reaction (12) when captured on protons emits only a 2.2 MeV photon. This is below the detection threshold of water detectors and hence they cannot normally tag the released neutron by delayed coincidence, as liquid scintillators can. However, things could change dramatically if GdCl_3 is dissolved into the water. Gadolinium has a large cross-section for neutron capture and the capture of neutron on Gadolinium releases a 8 MeV gamma cascade. This being above the energy threshold, could be easy to observe in water detectors [69], transforming them into giant $\bar{\nu}_e$ detectors with statistics many times the statistics expected in scintillator detectors. This could give exceptional sensitivity to neutrino oscillation parameters using reactor antineutrinos [112]. This will help also in DSNB detection by lowering the lower energy threshold, and we should be able to use the same energy window as in liquid scintillators. Following [55], we present our results for the energy range (10 – 30) MeV. The energy resolution of course continues to be given by Eq. (15).

2.3.4 Liquid Argon Detectors

Liquid argon TPCs are unique as they allow the detection of ν_e . The only other ν_e sensitive detector technology that we have so far seen built on a large scale was the heavy water detector at SNO. However, SNO is now dismantled. Significant amount of R&D on the other hand has

gone into the liquid argon option. The ICARUS detector [113] in Italy already consists of a 600 ton module and has shown the feasibility of this detector technology. Since it is one of the few detector types which can be built on a large scale and allows for very fine granularity, good electron detection efficiency as well as detection of τ events, this is often considered as a far detector option for the Neutrino Factory. Feasibility of probing galactic SN neutrinos was studied in [114, 115] and DSNB in [63, 62]. A future large liquid argon detector could have a mass of about 100 kton. Some of the currently pursued proposals include GLACIER [116], MODULAR [118] and FLARE [117]. Energy resolution in this detector is expected to be extremely good and at energies relevant for the neutrino factory it is believed to be in the ballpark of $\sigma_E \sim 0.03\sqrt{E}$ (GeV). Therefore, at energies relevant for DSNB, one can assume that the energy reconstruction could be almost perfect. In what follows, we work under this assumption and give our results in terms of the neutrino energy. Since further R&D would be needed to determine the backgrounds in this detector, we will show results for an energy window of (20 – 40) MeV.

3 Expected Events from DSNB

3.1 DSNB Antineutrino Events in Water and Scintillator Detectors

We give in this subsection the number of DSNB $\bar{\nu}_e$ events expected in water and scintillator detectors. The total expected number of events are presented in Table 3. The energy windows in which we have calculated the total number of events were discussed in the previous section and are shown in the parentheses in the first row of the table. The number of events per year have been calculated assuming a fiducial mass of 22.5 kton for SK and Gadolinium loaded SK (GDSK), 1 Mton for a future megaton detector (marked in the table symbolically as HK) and Gadolinium loaded megaton water detector (GDHK) and 50 kton for the scintillator detector (LENA). The results for NH remain the same for any value of θ_{13} . For IH the neutrino oscillation probability and hence the number of events depend on θ_{13} . We explicitly show results for two extreme values of θ_{13} – for small θ_{13} such that the jump probability $P_{13} = 1$ and for large θ_{13} such that the jump probability $P_{13} = 0$. For showcasing the impact of collective effects on the predictions for DSNB (anti)neutrino events, we also present in the Table 3 expected number of events if collective effects were not taken into account. These are shown in parenthesis. When there are no collective effects, one has only standard MSW transitions in the SN and it is well known that in this case antineutrinos undergo maximal flavor transitions for IH when θ_{13} is large ($P_{13} = 0$), while for small values of θ_{13} or with NH (for any θ_{13}) there is no matter enhanced resonant oscillations and these two scenarios give identical results. We therefore get larger number of events for IH and large θ_{13} . However, once the collective effects are switched on, the small and large θ_{13} cases of IH switch roles. Since there are now two stages of flavor conversions, first due to collective effects deep inside the SN and then due to MSW transitions, the final $\bar{\nu}_e$ fluxes are such that IH with large θ_{13} and NH give identical predictions, while IH with small θ_{13} predicts larger number of events (cf. upper right panel of Fig. 1).

It can be seen, that we expect about a couple of events per year in SK ⁴. This would go up by a

⁴Note that there will also be a large number of background events in the detector and one has to find the signal by looking at excess of events above the fluctuations in the background. This makes DSNB detection more difficult.

Model	Hierarchy	SK (19.3 - 30.0) (MeV)	GDSK (10.0 - 30.0) (MeV)	HK (19.3 - 30.0) (MeV)	GDHK (10.0 - 30.0) (MeV)	LENA (10.0 - 25.0) (MeV)
G1	NH	1.7 (1.7)	4.9 (4.9)	67.8 (67.8)	196.0 (196.0)	6.4 (6.4)
	IH ($P_{13} = 0$)	1.7 (2.7)	4.9 (7.4)	67.8 (109.6)	196.0 (296.0)	6.4 (9.5)
	IH ($P_{13} = 1$)	2.7 (1.7)	7.4 (4.9)	109.6 (67.8)	296.0 (196.0)	9.5 (6.4)
G2	NH	1.1 (1.1)	3.5 (3.5)	42.6 (42.6)	139.5 (139.5)	4.6 (4.6)
	IH ($P_{13} = 0$)	1.1 (1.5)	3.5 (5.1)	42.6 (58.5)	139.5 (205.7)	4.6 (6.9)
	IH ($P_{13} = 1$)	1.5 (1.1)	5.1 (3.5)	58.5 (42.6)	205.7 (139.5)	6.9 (4.6)
LL	NH	2.5 (2.5)	6.2 (6.2)	98.2 (98.2)	246.0 (246.0)	7.7 (7.7)
	IH ($P_{13} = 0$)	2.5 (4.4)	6.2 (8.9)	98.2 (175.7)	246.0 (356.0)	7.7 (10.6)
	IH ($P_{13} = 1$)	4.4 (2.5)	8.9 (6.2)	175.7 (98.2)	356.0 (246.0)	10.6 (7.7)

Table 3: Number of expected events per year per 22.5 kton of SK and GDSK, 1000 kton of HK and GDHK, and 50 kton of LENA. The events without collective effects are shown in parenthesis for comparison.

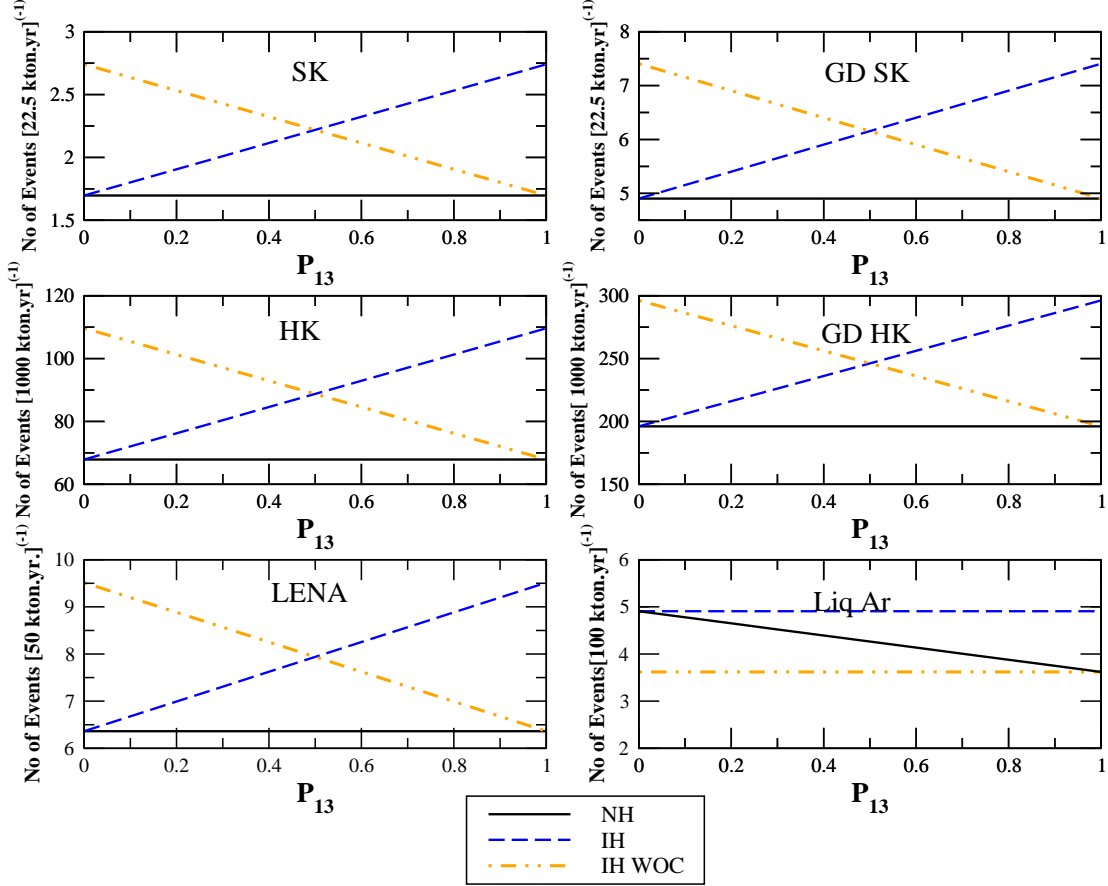


Figure 2: Number of expected events as a function of the jump probability P_{13} for the G1 model. Black lines are for NH and blue dashed lines for IH. The yellow dashed dotted lines show the case for IH without collective effects (WOC).

factor of about 2–3 if Gadolinium were to be added to the water. The corresponding number for a megaton of water would be scaled upwards by a factor of $1000/22.5$ and we expect about 40–176 (140–356) events per year in megaton water (Gadolinium loaded water) detectors depending on the choice of the neutrino mass hierarchy and θ_{13} and the SN model. After 10 years of running these numbers would be a factor of 10 higher, and we could have a few thousand events in the Gadolinium loaded detector. It should therefore be straightforward for megaton water detectors, with or without Gadolinium, to be able to observe these DSNB fluxes. More importantly we note that for a given SN flux model, it should be easy for megaton water detectors to determine the hierarchy, if $\sin^2 \theta_{13} \lesssim 10^{-5}$. For almost vanishing θ_{13} , we can see that for G1, NH predicts 1960 ± 44 (678 ± 26) events in 10 years of running of GDHK (HK) while IH predicts 2960 ± 54 (1096 ± 33). It would therefore be easy to distinguish one hierarchy from the other. Note that this is one of the very rare type of experiments which can give information about the neutrino mass hierarchy even if θ_{13} was below the reach of the most Neutrino Factory and Beta-beam experiments. A 50

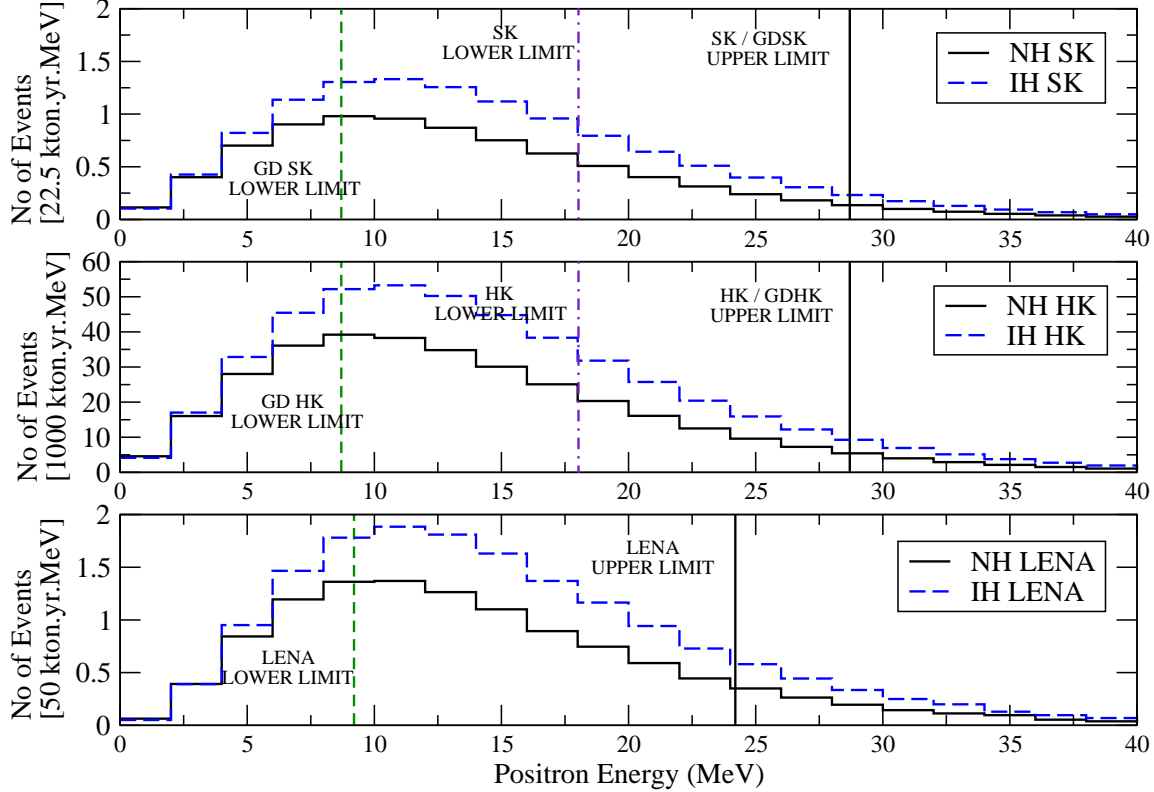


Figure 3: Number of expected events per year in 2 MeV positron energy bins in SK (upper panel) HK (middle panel) and LENA (lower panel). The solid black lines show the projected event spectrum for NH while the dashed blue lines are if IH was true with $P_{13} = 1$. The SN flux model corresponds to G1.

kton liquid scintillator detector should be able to record 46 – 106 events in 10 years of running.

We have shown in the Table, number of events expected assuming either the G1, G2 or LL model for the initial SN neutrino fluxes. We find that the lowest number of events are predicted by the G2 model, while LL predicts the highest event rate. In fact, one can see that the event rate predicted by NH and G1 is close to that predicted by IH and G2. Likewise, the rate predicted by IH and G1 is close to the one predicted by NH and LL. We have discussed before the uncertainty associated with the SN models. Therefore, if the uncertainty in the model predictions for the initial fluxes remain at the current level, then it might be hard to distinguish the hierarchy from the DSNB itself, especially in the smaller detectors. However, for Gadolinium loaded megaton water detectors it might still be possible to say something about the hierarchy. Also, for G2 and NH (LL and IH) we have a prediction which is lower (higher) than any other case and therefore for these cases there is no confusion. For instance, if GDHK records less (greater) than 1500 (3000)

	G1	G2	LL
NH ($P_{13} = 0$)	4.9 (4.9)	2.3 (2.3)	9.9 (9.9)
NH ($P_{13} = 1$)	3.6 (3.6)	1.7 (1.7)	7.3 (7.3)
IH	4.9 (3.6)	2.3 (1.7)	9.9 (7.3)

Table 4: Number of ν_e charged current events on ^{40}Ar per year per 100 kton of Liquid argon TPC in the energy window $E_\nu = (20 - 40)$ MeV. The events without collective effects are shown in parenthesis for comparison.

events, we could say that the hierarchy is normal (inverted). Of course, we have nowhere taken into account the uncertainty in the star formation rate. That might bring additional complication, which we do not address in this paper.

So far we have presented results only for two extreme cases of θ_{13} , very low corresponding to $P_{13} = 1$ and very high corresponding to $P_{13} = 0$. For intermediate values of the mixing angle the jump probability ranges between 0 and 1. We show in Fig. 2 how the total event rate in the different detectors change as a function of P_{13} . The SN model assumed is G1. Solid black lines show the case for NH while the dashed blue lines show the case for IH, where we have included both collective as well as MSW transitions inside the SN. It is easy to see from the expressions given in Table 2 that for IH, the event rate would rise almost linearly with P_{13} . If collective effects were not taken into account then the trend would have been the opposite, and we would see a decrease in the $\bar{\nu}_e$ event rate with P_{13} . These are shown for the different detectors by the yellow dot-dashed lines in the figure.

For sizable number of events, it might even be possible to do a spectral analysis of the DSNB events. We show in Fig. 3 the event spectrum for 22.5 kton SK (upper panel), 1 Mton HK (middle) and 50 kton LENA (lower panel). The events per year are shown in 2 MeV energy bins. The solid black lines give the event spectrum for NH while the blue dashed lines are for IH with $P_{13} = 1$. We show results where both collective as well as MSW oscillations are taken into account. Upper and lower energy threshold for the different cases are indicated by vertical lines and we have assumed the G1 model for the initial fluxes.

3.2 DSNB Neutrino Events in Liquid Argon Detectors

Liquid argon TPC could offer a unique laboratory to probe ν_e from a future galactic SN as well as from the DSNB around us. We show in Table 4 the number of expected ν_e charged current events

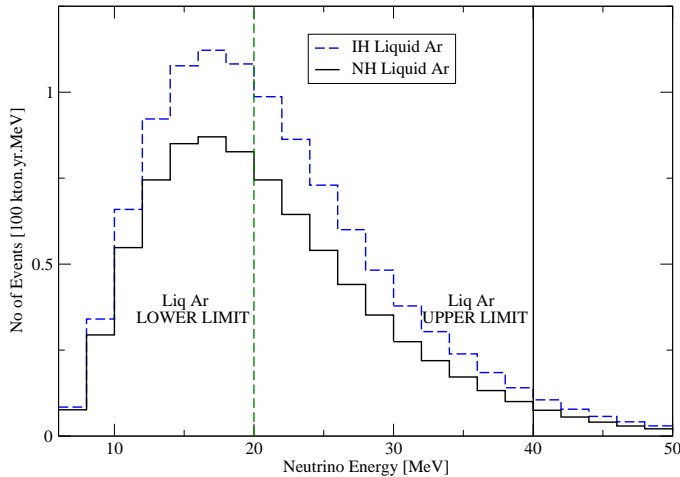


Figure 4: Number of expected events per year in 2 MeV neutrino energy bins in a 100 kton Liquid argon TPC. The solid black lines show the projected event spectrum for NH ($P_{13} = 1$) while the dashed blue lines are if IH was true. The SN flux model corresponds to G1.

on ^{40}Ar . We show results for NH and large θ_{13} ($P_{13} = 0$), NH and small θ_{13} ($P_{13} = 1$), and IH for any value of θ_{13} . Expected number of events are shown for the three benchmark flux models. We see that the number of ν_e events expected in liquid argon detectors is extremely small. This is because the $\nu_e + ^{40}\text{Ar} \rightarrow e^- + ^{40}\text{K}^*$ cross-section (taken from [115]) is very small at low energies and rises very fast as the energy increases. The DSNB flux on the other hand gets redshifted to lower energies thereby reducing the number of events. In particular, the DSNB flux is peaked at around 5 MeV, with very few neutrinos in the energy window 20–40 MeV (cf. Fig. 1). It might also be interesting to compare the number of expected ν_e events in a liquid argon detector, with the number of $\bar{\nu}_e$ events in a water detector, for same number of target nuclei/nucleons. It turns out that 100 kton of liquid argon has 1.5×10^{33} argon targets, while 22.5 kton water detector (SK) also has 1.5×10^{33} proton targets. On the other hand, the cumulative cross-section in the energy window of 20–40 MeV for ν_e capture on ^{40}Ar is larger than the cross-section for $\bar{\nu}_e$ capture on protons by a factor of about 2. Signal in this energy window, for the LL SN model with complete flavor conversion⁵, would be 9.9 and 5.8 events in 100 kton of liquid argon and 22.5 kton of water, respectively. This implies a ratio of about 1.7, which agrees with the rough estimate of the factor of 2 coming from the difference in the cross-sections. If we could lower the energy threshold in liquid argon to 5.5 MeV, we could expect about 8.1 events per year for NH with small θ_{13} and about 10.5 events per year for IH (and NH with large θ_{13}). In Fig. 4 we show the event spectrum in bins of 2 MeV width. The black solid line shows the spectrum for NH with $P_{13} = 1$ while the blue dashed line is for IH.

⁵For complete flavor conversion, the resultant flux at both liquid argon and water detector is ν_x , and is therefore the same. Of course in reality, complete flavor conversion can be possible only in one channel. The above example is just to illustrate the difference in the number of events for the two detector types being compared.

4 Summary and Conclusions

Neutrinos emitted by core-collapse supernovae over the entire history of the Universe, pervade us. This is the so-called diffuse supernova neutrino background. The DSNB fluxes are theoretically given by folding the neutrinos emitted from a typical SN with the rate of SN explosions as a function of the redshift, and integrating over all redshifts to take into account all possible SN explosions that might have happened in the Universe. Since the final fluxes emerging from the SN depend on neutrino flavor conversions inside the SN, the DSNB fluxes also depend very crucially on neutrino properties. Therefore, while a galactic SN event is eagerly awaited in order to shed light on SN theory on one hand and neutrino properties on the other, detecting the DSNB in currently running and future detectors could help us constrain SN dynamics, cosmic star formation rate as well as neutrino properties. However, the primary agenda is to successfully observe them in terrestrial detectors.

Being redshifted, the spectrum of DSNB fluxes is peaked at smaller energies, making their detection even more challenging. So far the running Super-Kamiokande detector has managed to put an upper bound on the $\bar{\nu}_e$ DSNB flux. However, the situation might improve in the future with possibility of a signal in the upcoming large scale detectors which would be built to serve as the far detector for high performance neutrino beam experiments. Observing DSNB would be free for these detectors and the physics output from that would be immense. In this paper we re-analyzed the potential of a selected class of future detectors to detect DSNB fluxes. Such an analysis has been warranted by the flurry of activity in the field of SN neutrino research, following the revival of interest in neutrino-neutrino self-interaction. These interactions inside the SN have been shown to produce significant change to the final neutrino flux spectrum, especially if the neutrino mass hierarchy is inverted. Since these so-called collective effects inside the SN are unavoidable, it was necessary to revisit the issue of DSNB detection.

We considered water, Gadolinium loaded water and liquid scintillator detectors for $\bar{\nu}_e$ DSNB detection and liquid argon TPC for observing the ν_e DSNB flux. A major issue in this field is the model uncertainties in the SN neutrino fluxes themselves. We presented results for three SN neutrino flux models. We calculated the total number of events for both the hierarchies and for two extreme values of θ_{13} resulting in jump probability $P_{13} \rightarrow 0$ and 1. Number of events expected in future megaton water and 50 kton liquid scintillator detectors are large, with a few thousand events expected in Gadolinium loaded megaton water detectors running for 10 years. For true inverted hierarchy, it becomes possible to get very large flavor oscillations even if $\theta_{13} \rightarrow 0$. We showed that under fortunate circumstances, it might be possible to get information on the neutrino mass hierarchy by observing DSNB in megaton water detectors. Note that this is a very unique situation, since for $\theta_{13} \rightarrow 0$ it becomes almost impossible to determine the hierarchy using long baseline experiments. In this way, DSNB detection could be complementary to the long baseline program. We also showed how the total number of events change if θ_{13} increases from very small to very large values, decreasing P_{13} from 1 to 0. Finally, we showed the event spectrum by binning the prospective data in 2 MeV bins.

In conclusion, very large number of DSNB events are expected in the next generation detectors and therefore, it should be possible to observe DSNB $\bar{\nu}_e$ in the future. Collective effects inside SN significantly change the predicted number of DSNB events if the hierarchy is inverted. Under fortunate conditions it might be possible to determine the neutrino mass hierarchy using the DSNB

signal and this could be done even if $\theta_{13} \rightarrow 0$, in which case long baseline experiments would not be able to tell the hierarchy at all. Prospects of DSNB detection look extremely promising and one might even feel optimistic about learning about neutrino oscillation parameters, cosmic star formation rate and maybe about SN physics, by observing these relic neutrinos in future detectors.

Acknowledgments

Authors wish to thank Manoj Kaplinghat for discussions during very early stages of this work, and the organizers of WHEPP X, during which this work was initiated. This work has been supported by the Neutrino Project under the XI Plan of Harish-Chandra Research Institute and the project 'Frontiers of Theoretical Physics' under the XI Plan of Saha Institute of Nuclear Physics. Basudeb Dasgupta acknowledges partial support from the Max Planck India Partnergroup at Tata Institute of Fundamental Research. Sovan Chakraborty would like to thank Harish-Chandra Research Institute for kind and warm hospitality. The authors thank Sebastian Galais and Christina Volpe for their critique of the previous version of this paper.

References

- [1] S. P. Mikheev and A. Y. Smirnov, Sov. Phys. JETP **64**, 4 (1986) [Zh. Eksp. Teor. Fiz. **91**, 7 (1986)] arXiv:0706.0454 [hep-ph].
- [2] G. M. Fuller, R. W. Mayle, J. R. Wilson, and D. N. Schramm "Resonant neutrino oscillations and stellar collapse," Astrophys. J. **322** 795 (1987).
- [3] A. S. Dighe and A. Y. Smirnov, Phys. Rev. D **62** (2000) 033007 arXiv:hep-ph/9907423.
- [4] C. Lunardini and A. Yu. Smirnov, JCAP **0306**, 009 (2003) arXiv:hep-ph/0302033.
- [5] A. S. Dighe, M. T. Keil and G. G. Raffelt, JCAP **0306**, 005 (2003) arXiv:hep-ph/0303210.
- [6] A. S. Dighe, M. T. Keil and G. G. Raffelt, JCAP **0306**, 006 (2003) arXiv:hep-ph/0304150.
- [7] A. S. Dighe, M. Kachelriess, G. G. Raffelt and R. Tomas, JCAP **0401**, 004 (2004) arXiv:hep-ph/0311172.
- [8] R. C. Schirato and G. M. Fuller, arXiv:astro-ph/0205390.
- [9] K. Takahashi, K. Sato, H. E. Dalhed and J. R. Wilson, Astropart. Phys. **20**, 189 (2003) arXiv:astro-ph/0212195.
- [10] G. L. Fogli, E. Lisi, A. Mirizzi, and D. Montanino, Phys. Rev. D **68**, 033005 (2003) arXiv:hep-ph/0304056.
- [11] R. Tomàs, M. Kachelrieß, G. Raffelt, A. Dighe, H. T. Janka and L. Scheck, JCAP **0409**, 015 (2004) arXiv:astro-ph/0407132.

- [12] G. L. Fogli, E. Lisi, A. Mirizzi and D. Montanino, JCAP **0504**, 002 (2005) arXiv:hep-ph/0412046.
- [13] V. Barger, P. Huber and D. Marfatia, Phys. Lett. B **617**, 167 (2005) arXiv:hep-ph/0501184.
- [14] B. Dasgupta and A. Dighe, Phys. Rev. D **75** (2007) 093002 arXiv:hep-ph/0510219.
- [15] S. Choubey, N. P. Harries and G. G. Ross, Phys. Rev. D **74**, 053010 (2006) arXiv:hep-ph/0605255.
- [16] G. L. Fogli, E. Lisi, A. Mirizzi and D. Montanino, JCAP **0606**, 012 (2006) arXiv:hep-ph/0603033.
- [17] A. Friedland and A. Gruzinov, arXiv:astro-ph/0607244.
- [18] S. Choubey, N. P. Harries and G. G. Ross, Phys. Rev. D **76**, 073013 (2007) arXiv:hep-ph/0703092.
- [19] J. P. Kneller, G. C. McLaughlin and J. Brockman, arXiv:0705.3835 [astro-ph].
- [20] R.M. Bionta et al., Phys. Rev. Lett. **58** (1987) 1494.
- [21] E.N. Alexeyev et al., JETP Lett. **45** (1987) 589.
- [22] K.S. Hirata et al., Phys. Rev. Lett. **58** (1987) 1490.
- [23] R. Diehl *et al.*, Nature **439**, 45 (2006) arXiv:astro-ph/0601015.
- [24] G. S. Bisnovatyi-Kogan and S. F. Seidov Annals N. Y. Acad. Sci. **422**, 319 (1984).
- [25] L. M. Krauss, S. L. Glashow and D. N. Schramm, Nature **310**, 191 (1984).
- [26] S. E. Woosley, J. R. Wilson and R. Mayle Astrophys. J. **302**, 19 (1986).
- [27] F. Mannucci, D. Maoz, K. Sharon, M. T. Botticella, M. Della Valle, A. Gal-Yam and N. Panagia, arXiv:0710.1094 [astro-ph].
- [28] Lilly S, Fèvre O L, Hammer F and Crampton D 1996 *Astrophys. J.* **460** L1
- [29] Madau P, Ferguson H C, Dickinson M E, Giavalisco M, Steidel C C and Fruchter A 1996 *Mon. Not. R. Astron. Soc.* **283** 1388
- [30] Cowie L, Songaila A, Hu E and Cohen J 1996 *Astron. J.* **112** 839
- [31] Connolly A, Szalay A, Dickinson M, Rao M S and Brunner R 1997 *Astrophys. J.* **486** L11
- [32] Sawicki M J, Lin H and Yee H K C 1997 *Astron. J.* **113** 1
- [33] Treyer M, Ellis R, Milliard B, Donas J and Bridges T 1998 *Mon. Not. R. Astron. Soc.* **300** 303

- [34] Madau P, Pozzetti L and Dickinson M 1998 *Astrophys. J.* **498** 106
- [35] Pascarelle S M, Lanzetta K M and Fernandez-Soto A 1998 *Astrophys. J.* **508** L1
- [36] Steidel C C, Adelberger K L, Giavalisco M, Dickinson M and Pettini M 1999 *Astrophys. J.* **519** 1
- [37] Hughes D H *et al.* 1998 *Nature* **394** 241
- [38] Flores H *et al.* 1999 *Astrophys. J.* **517** 148
- [39] Gallego J, Zamorano J, Aragón-Salamanca A and Rego M 1995 *Astrophys. J.* **455** L1
- [40] Gronwall C 1998 in: Thuan T *et al.* (eds), *Proc. 33rd Rencontres de Moriond, Dwarf Galaxies and Cosmology* (Gif-sur-Yvette: Editions Frontières) p 41
- [41] Tresse L and Maddox S 1998 *Astrophys. J.* **495** 691
- [42] Glazebrook K, Blake C, Economou F, Lilly S and Colless M 1999 *Mon. Not. R. Astron. Soc.* **306** 843
- [43] E. N. Archibald, J. S. Dunlop, D. H. Hughes, S. Rawlings, S. A. Eales and R. J. Ivison, *Mon. Not. Roy. Astron. Soc.* **323**, 417 (2001) arXiv:astro-ph/0002083.
- [44] Somerville R S, Primack J R and Faber S M 2001 *Mon. Not. R. Astron. Soc.* **320** 504
- [45] L. E. Strigari, J. F. Beacom, T. P. Walker and P. Zhang, *JCAP* **0504**, 017 (2005) arXiv:astro-ph/0502150.
- [46] A. Mirizzi and G. G. Raffelt, *Phys. Rev. D* **72**, 063001 (2005) arXiv:astro-ph/0508612.
- [47] R. Buras, H. -Th. Janka, M. T. Keil, G. G. Raffelt and M. Rampp, *Astrophys. J.* **587** (2003) 320 arXiv:astro-ph/0205006.
- [48] T. Totani, K. Sato, H. E. Dalhed and J. R. Wilson, *Astrophys. J.* **496** (1998) 216 arXiv:astro-ph/9710203.
- [49] R. A. Malaney, *Astropart. Phys.* **7** (1997) 125 arXiv:astro-ph/9612012.
- [50] D. H. Hartmann and S. E. Woosley, *Astropart. Phys.* **7** (1997) 137.
- [51] T. Totani, K. Sato and Y. Yoshii, *Astrophys. J.* **460** (1996) 303 arXiv:astro-ph/9509130.
- [52] M. Kaplinghat, G. Steigman and T. P. Walker, *Phys. Rev. D* **62** (2000) 043001 arXiv:astro-ph/9912391.
- [53] L. E. Strigari, M. Kaplinghat, G. Steigman and T. P. Walker, *JCAP* **0403** (2004) 007 arXiv:astro-ph/0312346.
- [54] M. Fukugita and M. Kawasaki, *Mon. Not. Roy. Astron. Soc.* **340** (2003) L7 arXiv:astro-ph/0204376.

- [55] M. Wurm, F. von Feilitzsch, M. Goeger-Neff, K. A. Hochmuth, T. M. Undagoitia, L. Oberauer and W. Potzel, *Phys. Rev. D* **75** (2007) 023007 arXiv:astro-ph/0701305.
- [56] S. Ando and K. Sato, *New J. Phys.* **6** (2004) 170 arXiv:astro-ph/0410061.
- [57] E. Cappellaro, M. Turatto, D. Y. Tsvetkov, O. S. Bartunov, C. Pollas, R. Evans and M. Hamuy, *Astron. Astrophys.* **322** (1997) 431 arXiv:astro-ph/9611191.
- [58] S. Ando, K. Sato and T. Totani, *Astropart. Phys.* **18** (2003) 307 arXiv:astro-ph/0202450.
- [59] S. Ando and K. Sato, *Phys. Lett. B* **559** (2003) 113 arXiv:astro-ph/0210502.
- [60] C. Lunardini, *Astropart. Phys.* **26** (2006) 190 arXiv:astro-ph/0509233.
- [61] S. Ando, *Astrophys. J.* **607** (2004) 20 arXiv:astro-ph/0401531.
- [62] C. Volpe and J. Welzel, arXiv:0711.3237 [astro-ph].
- [63] A. G. Cocco, A. Ereditato, G. Fiorillo, G. Mangano and V. Pettorino, *JCAP* **0412**, 002 (2004) arXiv:hep-ph/0408031.
- [64] J. F. Beacom and L. E. Strigari, *Phys. Rev. C* **73** (2006) 035807 arXiv:hep-ph/0508202.
- [65] C. Lunardini, *Phys. Rev. D* **73** (2006) 083009 arXiv:hep-ph/0601054.
- [66] M. Aglietta *et al.*, *Astropart. Phys.* **1** (1992) 1.
- [67] M. Malek *et al.* [Super-Kamiokande Collaboration], *Phys. Rev. Lett.* **90** (2003) 061101 arXiv:hep-ex/0209028.
- [68] C. Lunardini and O. L. G. Peres, arXiv:0805.4225 [astro-ph].
- [69] J. F. Beacom and M. R. Vagins, *Phys. Rev. Lett.* **93**, 171101 (2004) arXiv:hep-ph/0309300.
- [70] J. T. Pantaleone, *Phys. Lett. B* **287**, 128 (1992).
- [71] S. Samuel, *Phys. Rev. D* **48**, 1462 (1993).
- [72] G. Sigl and G. Raffelt, *Nucl. Phys. B* **406**, 423 (1993).
- [73] Y. Z. Qian and G. M. Fuller, *Phys. Rev. D* **51**, 1479 (1995) arXiv:astro-ph/9406073.
- [74] V. A. Kostelecky and S. Samuel, *Phys. Rev. D* **52**, 621 (1995) arXiv:hep-ph/9506262.
- [75] S. Pastor, G. G. Raffelt and D. V. Semikoz, *Phys. Rev. D* **65**, 053011 (2002) arXiv:hep-ph/0109035.
- [76] H. Duan, G. M. Fuller and Y. Z. Qian, *Phys. Rev. D* **74**, 123004 (2006) arXiv:astro-ph/0511275.
- [77] H. Duan, G. M. Fuller, J. Carlson and Y. Z. Qian, *Phys. Rev. D* **74**, 105014 (2006) arXiv:astro-ph/0606616.

- [78] S. Hannestad, G. G. Raffelt, G. Sigl and Y. Y. Y. Wong, Phys. Rev. D **74**, 105010 (2006) [Erratum-ibid. D **76**, 029901 (2007)] arXiv:astro-ph/0608695.
- [79] H. Duan, G. M. Fuller, J. Carlson and Y. Z. Qian, Phys. Rev. D **75**, 125005 (2007) arXiv:astro-ph/0703776.
- [80] G. G. Raffelt and A. Y. Smirnov, Phys. Rev. D **76**, 081301 (2007) [Erratum-ibid. D **77**, 029903 (2008)] arXiv:0705.1830 [hep-ph].
- [81] A. Esteban-Pretel, S. Pastor, R. Tomas, G. G. Raffelt and G. Sigl, Phys. Rev. D **76**, 125018 (2007) arXiv:0706.2498 [astro-ph].
- [82] H. Duan, G. M. Fuller and Y. Z. Qian, Phys. Rev. D **76**, 085013 (2007) arXiv:0706.4293 [astro-ph].
- [83] G. G. Raffelt and A. Y. Smirnov, Phys. Rev. D **76**, 125008 (2007) arXiv:0709.4641 [hep-ph].
- [84] H. Duan, G. M. Fuller, J. Carlson and Y. Q. Zhong, Phys. Rev. Lett. **99**, 241802 (2007) arXiv:0707.0290 [astro-ph].
- [85] G. L. Fogli, E. Lisi, A. Marrone and A. Mirizzi, JCAP **0712**, 010 (2007) arXiv:0707.1998 [hep-ph].
- [86] H. Duan, G. M. Fuller, J. Carlson and Y. Z. Qian, Phys. Rev. Lett. **100**, 021101 (2008) arXiv:0710.1271 [astro-ph].
- [87] A. Esteban-Pretel, S. Pastor, R. Tomas, G. G. Raffelt and G. Sigl, Phys. Rev. D **77**, 065024 (2008) arXiv:0712.1137 [astro-ph].
- [88] C. Lunardini, B. Mueller and H. T. Janka, arXiv:0712.3000 [astro-ph].
- [89] B. Dasgupta and A. Dighe, arXiv:0712.3798 [hep-ph].
- [90] H. Duan, G. M. Fuller and Y. Z. Qian, arXiv:0801.1363 [hep-ph].
- [91] B. Dasgupta, A. Dighe, A. Mirizzi and G. G. Raffelt, arXiv:0801.1660 [hep-ph].
- [92] B. Dasgupta, A. Dighe and A. Mirizzi, arXiv:0802.1481 [hep-ph].
- [93] J. Dunkley *et al.* [WMAP Collaboration], arXiv:0803.0586 [astro-ph].
- [94] A.M. Hopkins and J.F. Beacom, Astrophys. J. **651**, 142 (2006).
- [95] M.D. Kistler et al, arXiv:0709.0381v2 [astro-ph].
- [96] I.K. Baldry and K. Glazebrook, Astrophys. J. **593**, 258 (2003).
- [97] P. Bhattacharjee, S. Chakraborty, S. Das Gupta, K. Kar, Phys. Rev. D **77**, 043008 (2008) arXiv:0710.5922v3 [astro-ph].

- [98] M. T. Keil, G. G. Raffelt and H. T. Janka, *Astrophys. J.* **590**, 971 (2003) arXiv:astro-ph/0208035.
- [99] B. Dasgupta, A. Dighe, G. G. Raffelt and A. Y. Smirnov, arXiv:0904.3542 [hep-ph].
- [100] <http://www.snolab.ca/public/science/index.html>
- [101] Y. Itow *et al.*, arXiv:hep-ex/0106019.
- [102] A. de Bellefon *et al.*, arXiv:hep-ex/0607026.
- [103] C. K. Jung, *AIP Conf. Proc.* **533**, 29 (2000).
- [104] S. Abe *et al.* [KamLAND Collaboration], arXiv:0801.4589 [hep-ex].
- [105] B. Aharmim *et al.* [SNO Collaboration], *Phys. Rev. C* **72**, 055502 (2005) arXiv:nucl-ex/0502021.
- [106] J. Engel, E. Kolbe, K. Langanke and P. Vogel, *Phys. Rev. C* **54**, 2740 (1996) arXiv:nucl-th/9606031; E. Kolbe, F. K. Thielemann, K. Langanke and P. Vogel, *Phys. Rev. C* **52**, 3437 (1995); E. Kolbe, K. Langanke and S. Krewald, *Phys. Rev. C* **49**, 1122 (1994).
- [107] J. F. Beacom, W. M. Farr and P. Vogel, *Phys. Rev. D* **66**, 033001 (2002) arXiv:hep-ph/0205220.
- [108] L. Cadonati, F. P. Calaprice and M. C. Chen, *Astropart. Phys.* **16**, 361 (2002) arXiv:hep-ph/0012082.
- [109] A. Bandyopadhyay, S. Choubey, S. Goswami and K. Kar, arXiv:hep-ph/0312315.
- [110] C. Arpesella *et al.* [Borexino Collaboration], *Phys. Lett. B* **658**, 101 (2008) arXiv:0708.2251 [astro-ph].
- [111] J. G. Learned, S. T. Dye and S. Pakvasa, *Prepared for 12th International Workshop on Neutrinos Telescopes: Twenty Years after the Supernova 1987A Neutrino Bursts Discovery, Venice, Italy, 6-9 Mar 2007*
- [112] S. Choubey and S. T. Petcov, *Phys. Lett. B* **594**, 333 (2004) arXiv:hep-ph/0404103.
- [113] P. Aprili *et al.* [ICARUS Collaboration], CERN-SPSC-2002-027 (2002).
- [114] I. Gil-Botella and A. Rubbia, *JCAP* **0408**, 001 (2004) arXiv:hep-ph/0404151; A. Bueno, I. Gil-Botella and A. Rubbia, arXiv:hep-ph/0307222.
- [115] I. Gil-Botella and A. Rubbia, *JCAP* **0310**, 009 (2003) arXiv:hep-ph/0307244;
- [116] A. Rubbia, arXiv:hep-ph/0402110; <http://neutrino.ethz.ch/GLACIER/Welcome.html>
- [117] www-off-axis.fnal.gov/flare/
- [118] B. Baibussinov *et al.*, *Astropart. Phys.* **29**, 174 (2008) arXiv:0704.1422 [hep-ph].